https://doi.org/10.5194/acp-2021-560
Preprint. Discussion started: 22 July 2021

Atmospheric Chemistry and Physics Discussions

Synergetic effects of NH_3 and NOx on the production and optical absorption of secondary organic aerosol formation from toluene photooxidation

Shijie Liu [a], Dandan Huang [b], Yiqian Wang [a], Si Zhang [a], Can Wu [a], Wei Du [a], Gehui Wang [a,c,*]

[a] Key Lab of Geographic Information Science of the Ministry of Education, School of Geographic Sciences, East China Normal University, Shanghai 210062, China

[b] State Environmental Protection Key Laboratory of Formation and Prevention of the Urban Air Pollution Complex, Shanghai Academy of Environmental Sciences, Shanghai 200233, China

[c] Institute of Eco-Chongming, 3663 North Zhongshan Road, Shanghai 200062, China

Corresponding author: Prof. Gehui Wang, e-mail: ghwang@geo.ecnu.edu.cn

https://doi.org/10.5194/acp-2021-560
Preprint. Discussion started: 22 July 2021

Atmospheric Chemistry and Physics Discussions

Abstract

NH_3 is the most important alkaline gas in the atmosphere and one of the key species affecting the behaviors of atmospheric aerosols. However, the impact of NH_3 on secondary organic aerosol (SOA) formation remains poorly understood, especially the dynamic evolution of chemical compositions in the SOA formation process. A series of chamber experiments was performed to probe the individual and common effects of NH_3 and NOx on toluene SOA formation through OH-photooxidation. The chemical compositions of toluene SOA were characterized using the Aerodyne high-resolution time-of-flight aerosol mass spectrometer (AMS). From 637 ± 14.6 μg m^{-3} (control), the SOA mass concentration increased to 867 ± 12.7 μg m^{-3} in the presence of NH_3 and decreased to 452 ± 18.9 μg m^{-3} in the presence of NOx. However, the highest SOA concentration (1020 ± 10.6 μg m^{-3}) and the lowest carbon oxidation state (OS_C) occurred in the presence of both NH_3 and NOx, indicating that the higher volatility products that formed in the presence of NOx could precipitate into the particle-phase when NH_3 was added. This resulted in a synergetic effect on SOA formation when NH_3 and NOx co-existed. The heterogeneous reaction was the main pathway by which NH_3 participated in SOA formation in the photooxidation process. The synergetic effect of NH_3 and NOx was also observed in SOA optical absorption. A peak at 280 nm, which is characteristic of organonitrogen imidazole compounds, was observed in the presence of NH_3 and its intensity increased when NOx was added into the chamber. This work improves our understanding of how the synergistic interactions between NH_3 and NOx influence SOA formation and offers new insights into mitigating aerosol pollution that

https://doi.org/10.5194/acp-2021-560
Preprint. Discussion started: 22 July 2021

Atmospheric Chemistry and Physics Discussions

45 factor in mixed atmospheric conditions.

46

47 **Keywords**: Photooxidation; Toluene; NH_3; Dynamic characteristics; Synergistic
48 effects

49

https://doi.org/10.5194/acp-2021-560
Preprint. Discussion started: 22 July 2021


Atmospheric Chemistry and Physics Discussions

1 Introduction

Secondary organic aerosols (SOA) are an important component of atmospheric particulate matter (Moise et al., 2015; Liu et al., 2017). SOA can significantly affect atmospheric visibility, air quality, and subsequently, public health (Paciga et al., 2014; Yang et al., 2016; Liu et al., 2017). The optical properties of aerosols have been directly and indirectly linked to their effects on the climate (Laskin et al., 2015; Xie et al., 2017; Peng et al., 2020). Because of the complexity of their chemical components, oxidation processes, and environmental factors, SOA formation mechanisms are very complex and the current understanding of SOA formation is incomplete. This limited understanding hampers the ability of models to predict the magnitudes, dynamics, and distributions of atmospheric aerosols from particulate and precursor emissions (Ortiz-Montalvo et al., 2014). In the past decades, although our understanding of SOA formation mechanisms has been constantly improving, there is still a gap between the simulated SOA concentration in large-scale atmospheric models and field observations (Volkamer et al., 2006; Yang et al., 2018).

Ammonia (NH_3) is the most important alkaline inorganic gas, it is widespread in the atmosphere and is one of the critical factors influencing SOA formation (Wang et al., 2018; Chen et al., 2019). Some studies have noted that the presence of NH_3 can contribute to the formation of more aerosol mass through photooxidation (Na et al., 2007; Li et al., 2018). Na et al. (2007) observed that aerosol yields in the α-pinene-ozone oxidation system increased by 8% when NH_3 was added. Li et al. (2018) concluded that the presence of NH_3 in the aromatic hydrocarbon photooxidation system

https://doi.org/10.5194/acp-2021-560
Preprint. Discussion started: 22 July 2021


Atmospheric Chemistry and Physics Discussions

72 increased aerosol size growth potentials (by 7%–108%), and resulted in enhanced SOA
73 formation. Qi et al. (2020) found that the concentration and average diameter of SOA
74 showed an immediate and rapid increase after adding NH_3. Furthermore, the acid-base
75 reactions between NH_3/NH_4^+ and the carboxyl groups in SOA molecules might enhance
76 SOA formation (Qi et al., 2020; Liu et al., 2015). The condensable ammonium salts
77 formed from the reaction between NH_3 and organic acids reduce the volatility of the
78 organic acids by several orders of magnitude (Paciga et al., 2014), and act as particle-
79 phase organics that further promote SOA formation (Na et al., 2007; Huang et al., 2012;
80 Chen et al., 2019; Qi et al., 2020). Along another pathway, glyoxal can undergo
81 nucleophilic attack by NH_3 through the Maillard reactions and form the corresponding
82 iminium intermediates (Nozière et al., 2009; Laskin et al., 2015; Liu et al., 2015). The
83 iminium intermediates can continue to react with carbonyls, which activates further
84 transformations such as the formation of heterocyclic compounds and oligomerization
85 reactions and forms condensation (oligomeric) products with more stable secondary
86 imines (Schiff bases) (Laskin et al., 2014). Both Nozière et al. (2009) and Ortiz-
87 Montalvo et al. (2014) reported NH_3 is an efficient catalyst for reactions with carbonyl
88 compounds to form nitrogen-containing compounds (NOCs). The reaction between
89 carbonyl and NH_3 can significantly decrease the volatility of oxidation products, which
90 further increases the yield of SOA (Lee et al., 2013; Zhang et al., 2015; Qi et al., 2020).
91 Babar et al. (2017) found that the substantial formation of secondary imines in the
92 presence of NH_3 was responsible for the higher α-pinene SOA yields. However, not all
93 studies have shown that the presence of NH_3 increases SOA yields. One study observed

https://doi.org/10.5194/acp-2021-560
Preprint. Discussion started: 22 July 2021


Atmospheric Chemistry and Physics Discussions

that NH_3 suppressed SOA formation under certain ozonation conditions (Ma et al., 2018b). Furthermore, the consumption of NH_3 by Criegee intermediates was reported to decrease the secondary ozonide yield and thus affect SOA formation.

Nitrogen oxides (NOx = NO + NO_2), which are mainly emitted from the combustion of fossil-fuels, have received significant attention due to their effects on the photooxidation process of volatile organic compounds (VOCs) and SOA formation (Draper et al., 2015; Berkemeier et al., 2016; Zhao et al., 2018; Surratt et al., 2006; Ng et al., 2007b; Sarrafzadeh et al., 2016). Laboratory experiments have found that SOA formation was initially enhanced, but then suppressed with increasing NOx concentrations (Sarrafzadeh et al., 2016; Yang et al., 2020). The competitive chemistry of organic peroxy radicals (RO_2) with hydroperoxyl radicals (HO_2) and NO was responsible for the variability in SOA formation (Xu et al., 2014; Ng et al., 2007a; Jiang et al., 2020). RO_2 mainly reacts with HO_2 under low-NOx conditions to form oxidation products with lower volatility, which may enable it to participated into the particle-phase and contribute to the SOA mass (Ng et al., 2007a). While the RO_2 + NO reaction is predominant in high-NOx conditions, the increase in volatile products formed through fragmentation was responsible for the decrease in SOA yield with increasing NOx (Zhao et al., 2018; Liu et al., 2019a; Xu et al., 2020). In addition, the suppressing effect of NOx on OH concentrations was another reason for the decreasing trend in SOA yields under high-NOx conditions (Sarrafzadeh et al., 2016).

In recent decades, atmospheric pollutants in China have changed significantly in their concentrations and composition (Wang et al., 2015; Xia et al., 2016). China

https://doi.org/10.5194/acp-2021-560
Preprint. Discussion started: 22 July 2021


Atmospheric Chemistry and Physics Discussions

decreased the emissions of SO_2 and NOx by 75% and 10% from 2007–2015 and from 2011–2015, respectively (de Foy et al., 2016; Vu et al., 2019; Wang et al., 2020). Owing to the lack of regulation regarding NH_3 emissions, NH_3 emissions increased by ~30 % from 2008–2016 over the North China Plain (Liu et al., 2018). As has been pointed out in previous research, the effect of NH_3 on the formation of SOA is one of gradual enhancement and may counteract any decreases in SOA formation due to reductions in SO_2 and NOx (Zhang et al., 2021). Indeed, one study observed that a reduction of NH_3 emissions improved $PM_{2.5}$ pollution compared to SO_2 in winter (Erisman and Schaap, 2004). Hence, the mechanism by which NH_3 affects SOA formation has attracted more and more attention. However, previous studies have not paid sufficient attention to the joint impacts of NH_3 and NOx on the formation of SOA and its corresponding optical properties. Due to the lack of real time detection methods for SOA chemical composition, the dynamic characteristics of how NH_3 participates in SOA formation via photooxidation have not been extensively studied.

Toluene is one of the most abundant aromatic VOCs in the urban atmosphere, which is also an important source of BrC (Ma et al., 2018a; Laskin et al., 2010). The effects of NH_3 and NOx on SOA formation through the toluene photooxidation process were investigated in this study. The chemical composition of toluene SOA was characterized on-line with an aerosol mass spectrometer and the dynamic characteristics of SOA chemical composition under different conditions were further explored by applying a positive matrix factorization (PMF) analysis. The optical properties of toluene SOA particles were determined based on a UV-vis spectrum

https://doi.org/10.5194/acp-2021-560
Preprint. Discussion started: 22 July 2021


Atmospheric Chemistry and Physics Discussions

138 analysis. Possible mechanisms of the effects of both NH_3 and NOx on SOA formation
139 were discussed. The results will help us to better understand SOA formation
140 mechanisms in complex pollution conditions with elevated NH_3 and NOx
141 concentrations in an urban atmospheric environment.

142

143 # 2 Materials and Methods

144 ## 2.1 Photooxidation chamber experiments

145 All toluene photooxidation experiments were performed in a 4 m^3 chamber. The
146 chamber has been described in detail in our previous studies. Briefly, the chamber was
147 constructed with a 0.08 mm-thick FEP-Teflon film. The average particle wall-loss rate
148 constant of 3.6×10^{-5} s^{-1} was used to correct the measured particle concentrations and
149 SOA yields in this study. 50 UV-B lamps (TUV36W, Philips) with peak wavelengths
150 of 254 nm were set up around the chamber and used as the light source to drive OH
151 radical formation through hydrogen peroxide (H_2O_2) photolysis. Mirror surfaced
152 stainless steel was used as the interior wall of the enclosure to maximize and
153 homogenize the interior light intensity.

154 Before each experiment, the chamber was flushed with zero air for at last 18 hours,
155 after which the concentration of particles was less than 1 cm^{-3}. Zero air was generated
156 by a zero air supply (111-D3N, Thermo Scientific™, USA). The flow rate of zero air
157 was controlled at 20 L min^{-1} by a mass flow controller (D088C/ZM, Beijing Sevenstar
158 Electron Corporation) during the process of inflating. The relative humidity (RH) of

https://doi.org/10.5194/acp-2021-560
Preprint. Discussion started: 22 July 2021


Atmospheric Chemistry and Physics Discussions

zero air was about 15~20%. For each experiment, measured amounts of toluene (Sigma-Aldrich, analytically pure) and H_2O_2 solution (Sigma-Aldrich, 30 wt% in H_2O) were injected into a Teflon bulb with micro syringes. Zero air was passed through the injection tube to make sure all the liquids had evaporated to the gas-phase and were blown into the chamber. NOx (Air Liquid Shanghai, 510 ppm NO_2 in N_2) and NH_3 (Air Liquid Shanghai, 502 ppm NH_3 in N_2) were introduced directly into the chamber to reach the required concentrations. For experiments with NOx, although only NO_2 was introduced into the chamber before photooxidation, NO could be formed through NO_2 photolysis under the UV light irradiation, so NO always coexisted with NO_2 in the photooxidation system (Zhao et al., 2018). Each experiment was performed without seed aerosols present. The experimental conditions for the toluene photooxidation are listed in Table 1.

2.2 Particle concentration measurements

For each experiment, a scanning mobility particle sizer (SMPS) was used to record the particle size distribution and volume concentration of the toluene-derived SOA. The SMPS was composed of a differential mobility analyzer (DMA model 3081, TSI Inc., USA) and a condensation particle counter (CPC model 3776, TSI Inc., USA) which were used for screening particles with specific aerodynamic equivalent sizes and for counting the number of the selected particles, respectively. The sheath gas velocity was 3 L min^{-1} and the sample gas velocity was 0.3 L min^{-1}. The scan was repeated every 5 min. During each scan circle, the scan time was 240 s, and the particle sizes ranged

https://doi.org/10.5194/acp-2021-560
Preprint. Discussion started: 22 July 2021


Atmospheric Chemistry and Physics Discussions

from 13.6 nm to 726.5 nm. A density of 1.4 g m^{-3}, which was measured by Ng et al. (2007), was used for the calculation of toluene SOA mass concentration from the particle volume concentration (Ng et al., 2007b).

2.3 Chemical characterization

In this study, the toluene SOA chemical compositions were characterized with an on-line high-resolution time-of-flight aerosol mass spectrometer (HR-ToF-AMS, Aerodyne Research Inc. USA). The sample flow passed through a Nafion dryer and the RH of the sample gas was reduced to below 20% before entering the AMS. In the injection port, an aerodynamic lens focused particles with a vacuum aerodynamic diameter below 1 μm into a narrow beam. Particles impacted a flash vaporizer (600°C) at the rear of the sizing region under high vacuum (~10^{-7} Torr) and were subsequently ionized by electron impact ionization (70 eV). Then, the positively charged ions entered the ToF section and were separated. V-mode (m/Δm = ~2000) was used in the AMS ToF section to address the high signal-to-noise. The separated ion fragments were analyzed by a quadrupole mass spectrometer with scans from 1 to 300 m/z. The composition-dependent collection efficiency (CE) was applied to the data based on the methods established by Middlebrook et al. (2012). For mass concentration calculations, 1.1, 1.2, and 1.4 were applied as the default relative ionization efficiency (RIE) values of nitrate, sulfate, and organic compounds, respectively. The standard AMS data analysis software SQUIRREL 1.63B coupled with PIKA 1.23B in the Igor Pro (WaveMetrics, Inc., Portland, Oregon), which were retrieved from

https://doi.org/10.5194/acp-2021-560
Preprint. Discussion started: 22 July 2021


Atmospheric Chemistry and Physics Discussions

http://cires1.colorado.edu/jimenez-group/ToFAMSResources/ToFSoftware/, were used for the analysis of elemental ratios and the ion speciated compositions of toluene SOA in the chamber. Note that the elemental ratios (i.e., O/C, H/C, and N/C) and mass-to-carbon ratio (OM/OC) were all calculated using the Aiken-Ambient method for comparability with previous studies (Aiken et al., 2008). In order to further explore the changes in SOA chemical composition, a PMF of the high-resolution mass spectra was performed to determine the different organic aerosol (OA) factors during the toluene photooxidation process. We preformed the PMF analysis in the same way as Zhang et al. (2011), the details of which are provided in the supporting information.

2.4 Absorption measurements

The changes of absorption spectra and the absorbance of the toluene derived SOA under different conditions were determined using a UV spectrophotometer (UV-3600, Shimadzu, Japan) with a 1 cm cuvette. The SOA was collected from a 3 m^3 sample gas onto the 46.2 nm PTFE filter (Whatman^{TM}, UK). The collected SOA sample was dissolved in 5 mL of methanol (HPLC grade, > 99.8%) with 30 min of sonication. The filter extracts were filtered through 0.2 μm PTFE syringe filters to remove suspended insoluble particles. Before detection of the optical absorbance, a cuvette filled with pure methanol was scanned as a blank to provide a spectral background. The absorption was detected over the range of 200 to 800 nm with a resolution of 0.5 nm^{-1}. The light absorption coefficient of the particles at a specific wavelength λ (Abs_λ, M/m) was calculated according to Eq. R1:

https://doi.org/10.5194/acp-2021-560
Preprint. Discussion started: 22 July 2021

Atmospheric Chemistry and Physics Discussions

$$Abs_{\lambda}=(A_{\lambda}-A_{700})\cdot\frac{V_l}{V_a\cdot L}\cdot\ln(10) \quad (R1)$$

where, A_{700} is the background value of light absorption intensity, calculated as the average value of light absorption intensity from 695–705 nm to reduce the limits of error in measurement; V_l and V_a are the volumes of methanol with dissolved particles and sampled air, respectively; and L is the optical path length. Because Abs_{λ} was strongly dependent on the amount of SOA, all Abs_{λ} results were normalized based on the SOA mass collected on the filter. The normalized result was defined as the mass absorption coefficient (MAC, $m^2\ g^{-1}$), calculated using Eq. R2:

$$MAC_{\lambda}=\frac{Abs_{\lambda}}{M} \quad (R2)$$

where, M ($\mu g\ m^{-3}$) represents the concentration of methanol-soluble organic carbon.

3 Result and Discussion

3.1 SOA formation

In order to investigate the effect of NH_3 and NOx during SOA formation from toluene photooxidation, a control test was carried out. The SOA mass concentrations at different conditions are shown in Fig. 1. There was a noticeable increase in the SOA mass concentration in the presence of NH_3. The mass concentration of SOA increased from 637 ± 14.6 $\mu g\ m^{-3}$ without NH_3 to a maximum of 867 ± 12.7 $\mu g\ m^{-3}$ with 200 ppb NH_3, consistent with previous studies (Na et al., 2007; Qi et al., 2020). Previous studies attributed the enhancement of SOA to the formation of NOCs from acid-base reactions between NH_3/NH_4^+ and carboxyl groups, or Maillard reactions of NH_3/NH_4^+ with

https://doi.org/10.5194/acp-2021-560
Preprint. Discussion started: 22 July 2021


Atmospheric Chemistry and Physics Discussions

241 carbonyl functional groups (Nozière et al., 2009; Ortiz-Montalvo et al., 2014; Liu et al.,
242 2015; Qi et al., 2020). In contrast, SOA concentrations were lower in the presence of
243 NOx, and the maximum mass concentration of toluene SOA was only 452 ± 18.9 μg m^{-3}
244 with 63 ppb initial NOx. Numerous studies have shown that, instead of RO_2 reacting
245 with RO_2/HO_2, NO would react with RO_2 to form the RO intermediate and produces
246 more oxidation products with higher volatilities through fragmentation in the presence
247 of NOx (Zhao et al., 2018; Liu et al., 2019a; Xu et al., 2020). Highly volatile compounds
248 cannot readily participate into the particle-phase, so this substantially suppresses the
249 formation of SOA.

250 The NOx and NH_3 had opposite effects on toluene SOA formation in this study.
251 Interestingly, however, the highest SOA mass concentration (1020 ± 10.6 μg m^{-3})
252 occurred in the presence of both NOx and NH_3, which was nearly 1.6 times higher than
253 that observed with no NOx or NH_3. Therefore, together NH_3 and NOx had a synergistic
254 effect on SOA formation because their combined effect on SOA formation was greater
255 than the sum of their separate effects. This may explain why predictions of SOA
256 concentrations in large-scale atmospheric models, which typically describe SOA
257 formation from data derived from chamber experiments, are frequently lower than field
258 observations (Volkamer et al., 2006). The effects of multiple factors are not well-
259 characterized by chamber experiments, which was partly responsible for the gap
260 between the simulations and field observations.

https://doi.org/10.5194/acp-2021-560
Preprint. Discussion started: 22 July 2021


Atmospheric Chemistry and Physics Discussions

3.2 SOA chemical composition

The traditional SOA formation mechanism is based on the chemical compositions obtained through off-line detection of the chemical composition of SOA (Jang et al., 2002; Liu et al., 2019a; Xu et al., 2020). SOA is dynamic and continually evolving in the atmosphere and the ageing process of SOA co-occurs with its formation process. Hence, the transformation of the SOA chemical composition during the SOA formation process is generally believed to be widespread, but is rarely characterized in the previous studies. Therefore, the AMS was used for on-line measurement of the SOA chemical composition and how the chemical composition evolved in the photooxidation process would be discussed in this section below.

The chemical composition of SOA is very complex. The average carbon oxidation state (OS_C) has been shown to be an ideal conceptual framework to describe changes in the degree of oxidation undergone by SOA (Kroll et al., 2011), and has been widely applied in field and laboratory studies (Chen et al., 2018; Mandariya et al., 2019). OS_C is calculated based on the measurements of O/C and H/C ($OS_C \approx 2 \times$ O:C - H:C). Fig. 2 shows the changes in the OS_C of toluene SOA formed in different experiments. Notably, all the toluene SOA was characterized as semi-volatile oxygenated organic aerosols (SV-OOA) with OS_C values ranging between -0.5 and 0. However, the different OS_C values and the change trends observed for the toluene SOA formed in different conditions (with and without NH_3/NOx) in Fig. 2 indicated that there was a

https://doi.org/10.5194/acp-2021-560
Preprint. Discussion started: 22 July 2021


Atmospheric Chemistry and Physics Discussions

281 photooxidation mechanism active during SOA formation, which ultimately changed the
282 SOA chemical compositions.

283 The OS_C increased over time for all SOAs that were formed in the absence of NH_3.
284 There are several possible reasons for the increasing trend of OS_C values. Firstly, a
285 dynamic equilibrium of semi-volatile vapors may have been achieved between the
286 particle-phase and gas-phase during the earlier toluene oxidation process. The increase
287 of SOA led to a reduction in the concentration of gas-phase semi-volatile organic
288 products. A decreasing concentration of gas-phase semi-volatile organic compound
289 products would suppress their transformation from gas-phase to particulate-phase.
290 More lower volatility gas-phase oxidation products with higher OS_C values would then
291 be shifted toward to the particle phase, which would be responsible for the continuing
292 increase of SOA. Secondly, the formed SOA could have been further oxidized by OH
293 through heterogeneous reactions (Kourtchev et al., 2015; Liu et al., 2019b). This could
294 be the main reason for the increase in the OS_C when the SOA concentration was no
295 longer increasing. Finally, even there was no OH in the chamber, the photodegradation
296 of SOA can produce oxygenated volatile organic compounds (OVOCs, e.g. acetic acid,
297 acetaldehyde, and acetone) under UV light irradiation, potentially leading to
298 measurable mass loss from SOA (Malecha and Nizkorodov, 2016). The
299 photoproduction of OVOCs from SOA had a lower OS_C than that of SOA, therefore,
300 the OS_C of SOA had increased to a certain extent.

301 The fact that additional photochemical processing results in the dynamic evolution
302 of the OS_C over time has been demonstrated in both field and laboratory experiments

https://doi.org/10.5194/acp-2021-560
Preprint. Discussion started: 22 July 2021


Atmospheric Chemistry and Physics Discussions

303 (Jimenez et al., 2009). The atmospheric oxidation of OA tends towards higher OS_C
304 regardless of the original OA source (Herndon et al., 2008). However, when NH_3 was
305 present, the OS_C of total SOA went almost unchanged for the whole photooxidation
306 period. Carboxy and carbonyl are the main oxygen-containing functional groups
307 responsible for the toluene photooxidation production (Ji et al., 2017). An organic
308 ammonium salt with four H atoms can offset an increase caused by the formation of
309 organic acids/carboxy group through acid-base reactions (Kuwata and Martin, 2012;
310 Liu et al., 2015). Or NH_3/NH_4^+ may react with carbonyl functional groups through
311 Maillard reactions, consuming the oxygen in the carbonyl group and leading to the
312 formation of species with covalent carbon-nitrogen bonds (Lee et al., 2013; Zhang et
313 al., 2015; Qi et al., 2020). Xu et al. (2018) showed that imidazole compounds (OSC ≈
314 -1.3) generated through heterogeneous reaction between NH_3 and carbonyl compounds
315 might contribute to the decrease in the OS_C of SOA. It is clear that an increase in OS_C
316 caused by the formation of oxygen-containing functional groups (e.g., carboxy,
317 carbonyl, etc.) would be counteracted through acid-base reactions or Maillard reactions
318 in the presence of NH_3. After 60 min of UV light irradiation, there was no more SOA
319 formation; however, the OS_C did decrease slightly, illustrating that the NH_3 could
320 continue to react with SOA through heterogeneous processes. Huang et al. (2016) also
321 pointed out that the portion of semi-volatile products with low OS_C formed at the later
322 stage of photooxidation also contributed to the decreased OS_C.

323 The OS_C of the toluene SOA formed with NOx was lower than that formed in the
324 absence of NOx, no matter whether NH_3 was present in the chamber or not. This

https://doi.org/10.5194/acp-2021-560
Preprint. Discussion started: 22 July 2021


Atmospheric Chemistry and Physics Discussions

325 indicated that an increased NOx concentration benefits the formation high volatility
326 oxidation products with lower OS_C values (Kroll et al., 2011; Jimenez et al., 2009).
327 However, the relationships between OS_C and SOA mass concentration with and without
328 NH_3 were the opposite of each other. Predictably, the SOA formation mechanism in the
329 presence of NOx is different from that with NOx + NH_3. In the absence of NH_3, the RO
330 intermediate, which is easily fragmented to produce relatively high-volatility
331 compounds, was the dominant product of the NOx + RO_2 reaction (Zhao et al., 2018;
332 Liu et al., 2019a; Xu et al., 2020). Highly volatile compounds cannot readily precipitate
333 into the particle-phase, which subsequently results in a lower SOA yield in the presence
334 of NOx (Yang et al., 2020). Thereby, both OS_C and the SOA mass concentration were
335 lower when 60 ppb NOx was added into the chamber. However, when both NOx and
336 NH_3 were present, the toluene derived SOA had the lowest OS_C value, but the highest
337 mass concentration. This result suggested that although NOx promotes the formation
338 of higher volatile compounds, these higher volatile compounds (e.g. glyoxal) can react
339 with NH_3 and precipitate into the particle-phase, which could contribute to the increase
340 in SOA formation. Huffman et al. (2009) observed that aerosol volatility was inversely
341 correlated with the extent of oxidation of OA components. The low value of OS_C in the
342 presence of NOx indicated that NOx would promote the formation of the relatively
343 high-volatility compounds. However, the lower OS_C value in the presence of NH_3
344 indicated that the high-volatility compounds would promote precipitation into the
345 particle-phase when reacting with NH_3.

346 Fragments derived from the AMS data have also been widely used to explore the

https://doi.org/10.5194/acp-2021-560
Preprint. Discussion started: 22 July 2021


Atmospheric Chemistry and Physics Discussions

bulk compositions and properties of SOA (Ng et al., 2010; Ng et al., 2017). The m/z 43 (f43) frequency was dominated by ion $C_2H_3O^+$, which is the tracer for organic compounds with alcohol and carbonyl functional groups (Alfarra et al., 2006). Meanwhile, the m/z 44 (f44) signal was dominated by CO_2^+ ions, which is the tracer for organic compounds with carboxyl functional groups and indicator of highly oxygenated organic aerosols (Ng et al., 2010). Here, we used f43 and f44 to express the fractions of $C_2H_3O^+$ and CO_2^+ to the total organic signal. The change of f43 *vs.* f44, which has an inflection point during the photooxidation process, is shown in Fig. 3. In our study, the change before the inflection point was defined as the formation stage, and the linear fit of f43 *vs.* f44 for the formation stage is shown by the dashed lines. The change in f43 *vs.* f44 after the inflection point was defined as the stable stage, and the linear fit of f43 *vs.* f44 in this stage is shown by the solid lines. The formation and stable stages of the f43 *vs.* f44 relationship during the experiment are discussed separately here.

In the stable stage, the increase in f44 and decrease in f43 with increasing OH exposure indicated that the carbonyl groups in toluene SOA were oxidized to carboxyl groups by the ageing process. For the experiments without NH_3 and NOx, the slope ratio of f43 *vs.* f44 was -3.9. When there was 60 ppb initial NOx, the f43 was almost stable while the f44 increased with the oxidation process. There was a lower slope ratio of f43 *vs.* f44, indicating that organic compounds with more alcohol and carbonyl functional groups had formed in the presence of NOx. But for the experiments with 200 ppb initial NH_3, the slope ratios of f43 *vs.* f44 were only -1.1 and -1.3 in the presence

https://doi.org/10.5194/acp-2021-560
Preprint. Discussion started: 22 July 2021


Atmospheric Chemistry and Physics Discussions

and absence of NOx, respectively. According to the above results, we can see that more carbonyl groups are consumed as carboxyl groups are formed in the presence of NH_3. The carbonyls can be oxidized to organic acids (Kawamura and Bikkina, 2016), but extra-consumed carbonyls can be nucleophilically attacked by NH_3/NH_4^+ to form nitrogen-heterocyclic compounds, e.g., imidazole (Grace et al., 2019; Lian et al., 2020). Meanwhile, the peak f44 value decreased from 0.13 to 0.10 when NH_3 was added into the chamber. This suggested that the heterogeneous reaction of NH_3/NH_4^+ could promote the consumption of particle-phase carbonyl groups (Xu et al., 2018), and must inhibit the formation of carboxyl groups in the SOA ageing process. The differences in spectra of toluene SOA in the formation stage and stable stage are shown in Fig. 4. A lower signal intensity variation of CO_2^+ in the presence of NH_3 also illustrated that NH_3 would inhibit heterogeneous reactions that form carboxyl groups.

In the formation stage, the slope ratios of f43 *vs.* f44 were almost the same for both experiments without NOx. It can thus be seen that the presence or absence of NH_3 does not affect the change trend of f43 *vs.* f44 in the SOA formation stage. Therefore, the gas-phase homogeneous reaction of NH_3 on SOA formation is not important. Clearly, the particle-phase heterogeneous reaction was the main reaction pathway by which NH_3 participated in the photooxidation process and toluene SOA formation. However, negative correlations were observed between f43 and f44 in the presence of NOx. Based on this, we concluded that NOx not only affects the SOA formation through the particle-phase heterogeneous reactions, but also through gas-phase homogeneous reactions.

https://doi.org/10.5194/acp-2021-560
Preprint. Discussion started: 22 July 2021


Atmospheric Chemistry and Physics Discussions

3.2 PMF results

A temporal evaluation of the toluene SOA chemical composition during photooxidation is vital to the analysis of the NOA formation mechanism in the presence of NH_3 and/or NOx. Therefore, this study further compared the chemical properties of the SOA generated under different experimental conditions by applying a PMF analysis to the HR-ToF-AMS data (Chen et al., 2019). A summary of the PMF results is presented in Fig. S1-S4. For the toluene OH-photooxidation experiments where NOx or NH_3 were present, the PMF analysis identified two factors. High-nitrogen OA (Hi-NOA) was tentatively assigned to the high N/C values and low-nitrogen OA (Lo-NOA) to the low N/C values. Fig. 5 compares the H/C, O/C, and N/C values of Hi-NOA and Lo-NOA in each experiment. Fig. 6 exhibits the evolution of Hi-NOA and Lo-NOA during the photooxidation process as resolved from the PMF analysis of different initial NOx/NH_3 concentrations. While similar evolutionary trends were observed under different conditions, the relative intensities and the chemical compositions of these two factors in each experiment were not consistent.

For the toluene SOA formed under NH_3 conditions, both Lo-NOA and Hi-NOA had similar O/C values, which were fully oxygenated with an average of 0.74 ± 0.04 (Fig. 5a). These O/C values were comparable to the low-volatility oxygenated organic aerosols (LV-OOA) with an O/C value ranging from 0.6 to 1 (Jimenez et al., 2009). The main difference between these two OA sources was the N/C ratio. The N/C ratio of Hi-NOA (N/C = 0.032) was about three times higher than that of Lo-NOA (N/C = 0.010)

https://doi.org/10.5194/acp-2021-560
Preprint. Discussion started: 22 July 2021


Atmospheric Chemistry and Physics Discussions

411 (Fig. 5a). The evolution of these two OA sources during the photooxidation process is
412 shown in Fig. 6a. The components of toluene SOA were mostly Lo-NOA during the
413 initial phase of SOA formation, but Hi-NOA toluene SOA started forming after 10
414 minutes and continued to gradually increase. It was likely that the formation pathway
415 of Hi-NOA did not involve the reaction of NH_3 with organic matter in the homogeneous
416 gas phase. The Lo-NOA reached the maximum mass concentration after 30 min of
417 photooxidation, and then decreased. The trends of these two OA factors suggested that
418 the formed Lo-NOA was converted into something else in the particle-phase. As the
419 Lo-NOA decreased, the mass concentration of Hi-NOA gradually increased. Thus, the
420 Hi-NOA should be derived from the heterogeneous reaction of Lo-NOA with
421 NH_3/NH_4^+. With the gradual replacement of Lo-NOA by Hi-NOA, the ratio of [Hi-
422 NOA]/[Lo-NOA] stabilized at 5~6.

423 For the toluene SOA formed under NOx conditions, there was not a large
424 difference between the N/C ratios of Hi-NOA (N/C = 0.019) and Lo-NOA (N/C = 0.014)
425 (Fig. 5c). At the end of the NOx experiment, the ratio of [Hi-NOA]/[Lo-NOA] was only
426 3:2 (Fig. 6c). It follows that the contribution of the heterogeneous NOx reaction to the
427 N/C ratio of toluene SOA was not obvious. Therefore, the formation of NOCs in the
428 presence of NOx mainly occurred through gas-phase homogeneous reactions, which
429 was consistent with the results in section 3.3.

430 The changing trend of N/C with time in the presence of NH_3 was different to that
431 with NOx present. The evolutions of the N/C of SOA in different experiments are
432 shown in Fig. 7. In the presence of NH_3, the N/C value gradually increased throughout

https://doi.org/10.5194/acp-2021-560
Preprint. Discussion started: 22 July 2021


Atmospheric Chemistry and Physics Discussions

433 the photooxidation process. The increased N/C value in the photooxidation process was
434 attributed to the heterogeneous NH_3 reaction with SOA. But in the presence of NOx,
435 the N/C increased rapidly to its maximum value where it was stable for the rest of the
436 reaction. This could mean that the heterogeneous reaction of toluene SOA with NOx to
437 form NOCs was not as important as the gas-phase homogeneous reaction.

438 When both NOx and NH_3 were added into the chamber, the N/C ratios of Hi-NOA
439 and Lo-NOA were 0.062 and 0.29, respectively (Fig. 5b). The N/C ratio of Hi-NOA,
440 which was comparable to the recently isolated nitrogen-enriched OA value (0.053)
441 observed by Sun et al. (2011), was much higher than that observed in the experiments
442 with only NH_3 or NOx. It was even higher than the sum of the N/C ratios from both
443 Exp. 2 with NH_3 and Exp. 4 with NOx. In order to calculate the relative contributions
444 of NH_3 and NOx to N/C, it was assumed that the effects of NH_3 or NOx on the N/C
445 ratio in the Hi-NOA and Lo-NOA factors did not change among different experimental
446 conditions. For Lo-NOA, the contributions of NH_3 and NOx to the N/C value were
447 0.0126 and 0.0164, and their relative intensities were 43% and 57%, respectively. While
448 for the Hi-NOA, the contributions of NH_3 and NOx to the N/C values were 0.0404 and
449 0.216, and their relative intensities were 65% and 35%, respectively. For the experiment
450 with both NH_3 and NOx, the contribution of NH_3 to N/C was higher by 26%, and the
451 contribution of NOx to N/C was higher by 17% compared to the experiments with
452 single pollutants. The co-existence of NH_3 and NOx further enhanced the N/C value of
453 toluene SOA, indicating that a synergetic interaction between NH_3 and NOx further
454 enhanced organic nitrogen formation.

https://doi.org/10.5194/acp-2021-560
Preprint. Discussion started: 22 July 2021


Atmospheric Chemistry and Physics Discussions

3.4 Optical absorption

The optical characteristics of toluene SOA formed from different NH_3 and NOx conditions were investigated. The MAC of toluene derived SOA detected over the range of 200–600 nm are displayed in Fig. 8. Over the entire UV detection range, an increase in light absorption was observed when the toluene SOA formed in the presence of NOx or NH_3.

Looking at Fig. 8 in detail, we see that the MAC of toluene SOA formed with (red line) and without (black line) NH_3 overlapped at 250 nm, but when the UV wavelength exceeded 250 nm the MAC of the toluene SOA formed in the presence of NH_3 was higher. The red line reflects an obvious characteristic absorption peak at 270~280 nm, which was mainly due to the absorption of the $n\rightarrow\pi^*$ electronic transitions. The imidazole compounds were formed through the Maillard reactions between NH_3/NH_4^+ with carbonyl functional groups (Zhang et al., 2015). The C=N double bonds in the organonitrogen imidazole compounds can act as effective chromophores since both $\pi\rightarrow\pi^*$ and $n\rightarrow\pi^*$ transitions are chromatically active (Nguyen et al., 2013). The UV/visible spectrum of imine and pyrrole show broad bands at 270 nm (NIST, 2020), which was consistent with the UV absorption peak of the $n\rightarrow\pi^*$ band observed here. According to the AMS results, carbonyl was the main functional group of toluene SOA. The emergence of absorption peaks at 270~280 nm demonstrated that some organonitrogen imidazole compounds (e.g. imines and pyrrole) were formed through the heterogeneous reaction of toluene with NH_3. Meanwhile, the high-molecular weight

https://doi.org/10.5194/acp-2021-560
Preprint. Discussion started: 22 July 2021


Atmospheric Chemistry and Physics Discussions

nitrogen-containing organic species might have formed through Maillard reactions in the particle-phase (Wang et al., 2010). This was also a reason for the increase in SOA mass concentration in the presence of NH_3.

The green line in Fig. 8 represents the MAC value of toluene-derived SOA in the presence of NOx, which was also higher than the black line (control) throughout the UV detection range. When compared with the red line, the green line had no obvious characteristic peak at 280 nm, but it had higher absorbance in the range between 240 and 280 nm. This indicated that both NOx and NH_3 increased the absorbance of toluene SOA, while the chromophores generated from the reactions between toluene-derived SOA with either NH_3 or NOx did not behave in the same way.

The blue line in Fig. 8 represents the absorbance of toluene SOA formed in the presence of both NOx and NH_3. The MAC of toluene SOA formed in the presence of both NOx and NH_3 was higher than the toluene SOA formed in the presence of either NH_3 or NOx. There might have been a synergetic effect between NOx and NH_3 on the absorbance of toluene SOA. Considering that the mass concentration of toluene SOA formed in the presence of both NH_3 and NOx was the highest, as described in section 3.1, the co-existence of NH_3 and NOx may also result in the toluene SOA having stronger light absorption and atmospheric radiative forcing. We also noted a higher MAC value at 280 nm, which illustrated that the presence of NOx could promote the formation of imines and pyrrole in the photooxidation system of toluene with NH_3.

https://doi.org/10.5194/acp-2021-560
Preprint. Discussion started: 22 July 2021


Atmospheric Chemistry and Physics Discussions

4 Conclusion

Here we present the results of a study in which we characterized the mass concentrations, chemical compositions, and optical properties of SOA formed from the photooxidation of toluene under different NH_3 and NOx conditions. When compared with the control experiment, the SOA mass concentration data showed that the formation of toluene-derived SOA was enhanced in the presence of NH_3, through acid-base reactions between carboxyl groups or Maillard reactions with carbonyl compounds, but inhibited in the presence of NOx. Meanwhile, the mass concentration of toluene SOA formed in the presence of both NOx and NH_3 was higher than those formed under either NH_3 or NOx alone. This result indicated that there was a synergistic interaction between NH_3 and NOx that further enhanced toluene-derived SOA formation. At the same time, the lowest OS_C value was obtained when both NH_3 and NOx were present. We concluded that high volatile compounds, which were formed from toluene photooxidation in the presence of NOx, could react with NH_3 to form products with lower volatilities, and promoted the participation of these products into the particle-phase.

Synergetic effects of NH_3 and NOx on the formation of NOCs and the optical properties of SOA were also observed in this study. The heterogeneous reaction was responsible for the formation of NOCs in the presence of NH_3; meanwhile, an absorption peak at 270~280 nm, which is characteristic of imine and pyrrole, was observed. In contrast, the formation of NOCs caused by NOx alone was mainly due to a gas phase homogeneous reaction.

https://doi.org/10.5194/acp-2021-560
Preprint. Discussion started: 22 July 2021


Atmospheric Chemistry and Physics Discussions

519 In the actual atmosphere, NOx and NH_3 co-exist. Therefore, the findings presented
520 here clearly show that the synergetic effects of NOx and NH_3 should not be neglected.
521 In the meantime, our work provides a scientific basis for the consideration of synergistic
522 emission reductions of NH_3 and NOx under the compound pollution conditions, which
523 will contribute to reducing the burden of aerosols in the atmosphere.

524

525 Data availability

526 The datasets are available upon request to the corresponding authors.

527

528 Author contributions

529 SL designed the experiment, conducted the experiments, performed the data
530 interpretation, and wrote the paper. DH performed the data interpretation and wrote the
531 paper. GW wrote the paper. YW, SZ, CW, WD contributed to the paper with useful
532 scientific discussions or comments.

533

534 Competing interests

535 The authors declare that they have no conflict of interest.

536

537 Acknowledgements

538 This work was financially supported by National Key Research and Development
539 Plan programs (Grant No. 2017YFC0212703); National Natural Science Foundation of

https://doi.org/10.5194/acp-2021-560
Preprint. Discussion started: 22 July 2021

China (Grant No.41773117, 42005088); the China Postdoctoral Science Foundation (Grant No. 2019M661427); Fundamental Research Funds for the Central Universities, Director's Fund of Key Laboratory of Geographic Information Science (Ministry of Education), East China Normal University (Grant No. KLGIS2021C02); amd ECNU Happiness Flower Program.

Reference

Alfarra, M. R., Paulsen, D., Gysel, M., Garforth, A. A., Dommen, J., Prevot, A. S. H., Worsnop, D. R., Baltensperger, U., and Coe, H.: A mass spectrometric study of secondary organic aerosols formed from the photooxidation of anthropogenic and biogenic precursors in a reaction chamber, Atmos. Chem. Phys., 6, 5279-5293, DOI 10.5194/acp-6-5279-2006, 2006.

Babar, Z. B., Park, J.-H., and Lim, H.-J.: Influence of NH_3 on secondary organic aerosols from the ozonolysis and photooxidation of α-pinene in a flow reactor, Atmos. Environ., 164, 71-84, 10.1016/j.atmosenv.2017.05.034, 2017.

Berkemeier, T., Ammann, M., Mentel, T. F., Poschl, U., and Shiraiwa, M.: Organic nitrate contribution to new particle formation and growth in secondary organic aerosols from α-pinene ozonolysis, Environ. Sci. Technol., 50, 6334-6342, 10.1021/acs.est.6b00961, 2016.

Chen, C. L., Li, L. J., Tang, P., and Cocker, D. R.: SOA formation from photooxidation of naphthalene and methylnaphthalenes with m-xylene and surrogate mixtures, Atmos. Environ., 180, 256-264, 10.1016/j.atmosenv.2018.02.051, 2018.

Chen, T. Z., Liu, Y. C., Ma, Q. X., Chu, B. W., Zhang, P., Liu, C. G., Liu, J., and He, H.: Significant source of secondary aerosol: formation from gasoline evaporative emissions in the presence of SO_2 and NH_3, Atmos. Chem. Phys., 19, 8063-8081, 10.5194/acp-19-8063-2019, 2019.

de Foy, B., Lu, Z., and Streets, D. G.: Satellite NO_2 retrievals suggest China has exceeded its NOx reduction goals from the twelfth Five-Year Plan, Sci. Rep., 6, 35912, 10.1038/srep35912, 2016.

Draper, D. C., Farmer, D. K., Desyaterik, Y., and Fry, J. L.: A qualitative comparison of secondary organic aerosol yields and composition from ozonolysis of monoterpenes at varying concentrations of NO_2, Atmos. Chem. Phys., 15, 12267-12281, 10.5194/acp-15-12267-2015, 2015.

Erisman, J. W., and Schaap, M.: The need for ammonia abatement with respect to secondary PM reductions in Europe, Environ. Pollut., 129, 159-163, 10.1016/j.envpol.2003.08.042, 2004.

Grace, D. N., Sharp, J. R., Holappa, R. E., Lugos, E. N., Sebold, M. B., Griffith, D. R., Hendrickson,

https://doi.org/10.5194/acp-2021-560
Preprint. Discussion started: 22 July 2021

572 H. P., and Galloway, M. M.: Heterocyclic product formation in aqueous brown carbon systems,
573 Acs Earth Space Chem, 3, 2472-2481, 10.1021/acsearthspacechem.9b00235, 2019.

574 Herndon, S. C., Onasch, T. B., Wood, E. C., Kroll, J. H., Canagaratna, M. R., Jayne, J. T., Zavala,
575 M. A., Knighton, W. B., Mazzoleni, C., Dubey, M. K., Ulbrich, I. M., Jimenez, J. L., Seila, R., de
576 Gouw, J. A., de Foy, B., Fast, J., Molina, L. T., Kolb, C. E., and Worsnop, D. R.: Correlation of
577 secondary organic aerosol with odd oxygen in Mexico City, Geophys. Res. Lett., 35, Artn L15804,
578 10.1029/2008gl034058, 2008.

579 Huang, D. D., Zhang, X., Dalleska, N. F., Lignell, H., Coggon, M. M., Chan, C. M., Flagan, R. C.,
580 Seinfeld, J. H., and Chan, C. K.: A note on the effects of inorganic seed aerosol on the oxidation
581 state of secondary organic aerosol-α-Pinene ozonolysis, J. Geophys. Res.-Atmos., 121, 12476-
582 12483, 10.1002/2016jd025999, 2016.

583 Huang, Y., Lee, S. C., Ho, K. F., Ho, S. S. H., Cao, N. Y., Cheng, Y., and Gao, Y.: Effect of ammonia
584 on ozone-initiated formation of indoor secondary products with emissions from cleaning products,
585 Atmos. Environ., 59, 224-231, 10.1016/j.atmosenv.2012.04.059, 2012.

586 Huffman, J. A., Docherty, K. S., Mohr, C., Cubison, M. J., Ulbrich, I. M., Ziemann, P. J., Onasch,
587 T. B., and Jimenez, J. L.: Chemically-resolved volatility measurements of organic aerosol fom
588 different sources, Environ Sci Technol, 43, 5351-5357, 10.1021/es803539d, 2009.

589 Jang, M., Czoschke, N. M., Lee, S., and Kamens, R. M.: Heterogeneous atmospheric aerosol
590 production by acid-catalyzed particle-phase reactions, Science, 298, 814-817,
591 10.1126/science.1075798, 2002.

592 Ji, Y., Zhao, J., Terazono, H., Misawa, K., Levitt, N. P., Li, Y., Lin, Y., Peng, J., Wang, Y., Duan, L.,
593 Pan, B., Zhang, F., Feng, X., An, T., Marrero-Ortiz, W., Secrest, J., Zhang, A. L., Shibuya, K.,
594 Molina, M. J., and Zhang, R.: Reassessing the atmospheric oxidation mechanism of toluene, Proc.
595 Natl. Acad. Sci. U. S. A., 114, 8169-8174, 10.1073/pnas.1705463114, 2017.

596 Jiang, X. T., Lv, C., You, B., Liu, Z. Y., Wang, X. F., and Du, L.: Joint impact of atmospheric SO_2
597 and NH_3 on the formation of nanoparticles from photo-oxidation of a typical biomass burning
598 compound, Environ Sci-Nano, 7, 2532-2545, 10.1039/d0en00520g, 2020.

599 Jimenez, J. L., Canagaratna, M. R., Donahue, N. M., Prevot, A. S., Zhang, Q., Kroll, J. H., DeCarlo,
600 P. F., Allan, J. D., Coe, H., Ng, N. L., Aiken, A. C., Docherty, K. S., Ulbrich, I. M., Grieshop, A.
601 P., Robinson, A. L., Duplissy, J., Smith, J. D., Wilson, K. R., Lanz, V. A., Hueglin, C., Sun, Y. L.,
602 Tian, J., Laaksonen, A., Raatikainen, T., Rautiainen, J., Vaattovaara, P., Ehn, M., Kulmala, M.,
603 Tomlinson, J. M., Collins, D. R., Cubison, M. J., Dunlea, E. J., Huffman, J. A., Onasch, T. B.,
604 Alfarra, M. R., Williams, P. I., Bower, K., Kondo, Y., Schneider, J., Drewnick, F., Borrmann, S.,
605 Weimer, S., Demerjian, K., Salcedo, D., Cottrell, L., Griffin, R., Takami, A., Miyoshi, T.,
606 Hatakeyama, S., Shimono, A., Sun, J. Y., Zhang, Y. M., Dzepina, K., Kimmel, J. R., Sueper, D.,
607 Jayne, J. T., Herndon, S. C., Trimborn, A. M., Williams, L. R., Wood, E. C., Middlebrook, A. M.,
608 Kolb, C. E., Baltensperger, U., and Worsnop, D. R.: Evolution of organic aerosols in the
609 atmosphere, Science, 326, 1525-1529, 10.1126/science.1180353, 2009.

610 Kawamura, K., and Bikkina, S.: A review of dicarboxylic acids and related compounds in
611 atmospheric aerosols: Molecular distributions, sources and transformation, Atmos. Res., 170,

https://doi.org/10.5194/acp-2021-560
Preprint. Discussion started: 22 July 2021

140-160, 10.1016/j.atmosres.2015.11.018, 2016.

Kourtchev, I., Doussin, J. F., Giorio, C., Mahon, B., Wilson, E. M., Maurin, N., Pangui, E., Venables, D. S., Wenger, J. C., and Kalberer, M.: Molecular composition of fresh and aged secondary organic aerosol from a mixture of biogenic volatile compounds: a high-resolution mass spectrometry study, Atmos. Chem. Phys., 15, 5683-5695, 10.5194/acp-15-5683-2015, 2015.

Kroll, J. H., Donahue, N. M., Jimenez, J. L., Kessler, S. H., Canagaratna, M. R., Wilson, K. R., Altieri, K. E., Mazzoleni, L. R., Wozniak, A. S., Bluhm, H., Mysak, E. R., Smith, J. D., Kolb, C. E., and Worsnop, D. R.: Carbon oxidation state as a metric for describing the chemistry of atmospheric organic aerosol, Nat. Chem., 3, 133-139, 10.1038/nchem.948, 2011.

Kuwata, M., and Martin, S. T.: Phase of atmospheric secondary organic material affects its reactivity, Proc. Natl. Acad. Sci. U. S. A., 109, 17354-17359, 10.1073/pnas.1209071109, 2012.

Laskin, A., Laskin, J., and Nizkorodov, S. A.: Chemistry of atmospheric brown carbon, Chem. Rev., 115, 4335-4382, 10.1021/cr5006167, 2015.

Laskin, J., Laskin, A., Roach, P. J., Slysz, G. W., Anderson, G. A., Nizkorodov, S. A., Bones, D. L., and Nguyen, L. Q.: High-resolution desorption electrospray ionization mass spectrometry for chemical characterization of organic aerosols, Anal. Chem., 82, 2048-2058, 10.1021/ac902801f, 2010.

Laskin, J., Laskin, A., Nizkorodov, S. A., Roach, P., Eckert, P., Gilles, M. K., Wang, B., Lee, H. J., and Hu, Q.: Molecular selectivity of brown carbon chromophores, Environ. Sci. Technol., 48, 12047-12055, 10.1021/es503432r, 2014.

Lee, A. K., Zhao, R., Li, R., Liggio, J., Li, S. M., and Abbatt, J. P.: Formation of light absorbing organo-nitrogen species from evaporation of droplets containing glyoxal and ammonium sulfate, Environ. Sci. Technol., 47, 12819-12826, 10.1021/es402687w, 2013.

Li, K., Chen, L., White, S. J., Yu, H., Wu, X., Gao, X., Azzi, M., and Cen, K.: Smog chamber study of the role of NH_3 in new particle formation from photo-oxidation of aromatic hydrocarbons, Sci. Total Environ., 619-620, 927-937, 10.1016/j.scitotenv.2017.11.180, 2018.

Lian, X., Zhang, G., Yang, Y., Lin, Q., Fu, Y., Jiang, F., Peng, L., Hu, X., Chen, D., Wang, X., Peng, P. a., Sheng, G., and Bi, X.: Evidence for the formation of imidazole from carbonyls and reduced nitrogen species at the individual particle level in the ambient atmosphere, Environ. Sci. Tech. Let., 10.1021/acs.estlett.0c00722, 2020.

Liu, M., Huang, X., Song, Y., Xu, T., Wang, S., Wu, Z., Hu, M., Zhang, L., Zhang, Q., Pan, Y., Liu, X., and Zhu, T.: Rapid SO2 emission reductions significantly increase tropospheric ammonia concentrations over the North China Plain, Atmos. Chem. Phys., 18, 17933-17943, 10.5194/acp-18-17933-2018, 2018.

Liu, S. J., Jia, L., Xu, Y., Tsona, N. T., Ge, S. S., and Du, L.: Photooxidation of cyclohexene in the presence of SO_2: SOA yield and chemical composition, Atmos. Chem. Phys., 17, 13329-13343, 10.5194/acp-17-13329-2017, 2017.

Liu, S. J., Jiang, X. T., Tsona, N. T., Lv, C., and Du, L.: Effects of NOx, SO_2 and RH on the SOA

https://doi.org/10.5194/acp-2021-560
Preprint. Discussion started: 22 July 2021


Atmospheric Chemistry and Physics Discussions

formation from cyclohexene photooxidation, Chemosphere, 216, 794-804, 10.1016/j.chemosphere.2018.10.180, 2019a.

Liu, S. J., Tsona, N. T., Zhang, Q., Jia, L., Xu, Y. F., and Du, L.: Influence of relative humidity on cyclohexene SOA formation from OH photooxidation, Chemosphere, 231, 478-486, 10.1016/j.chemosphere.2019.05.131, 2019b.

Liu, Y. C., Liggio, J., Staebler, R., and Li, S. M.: Reactive uptake of ammonia to secondary organic aerosols: kinetics of organonitrogen formation, Atmos. Chem. Phys., 15, 13569-13584, 10.5194/acp-15-13569-2015, 2015.

Ma, P., Zhang, P., Shu, J., Yang, B., and Zhang, H.: Characterization of secondary organic aerosol from photo-oxidation of gasoline exhaust and specific sources of major components, Environ. Pollut., 232, 65-72, 10.1016/j.envpol.2017.09.018, 2018a.

Ma, Q., Lin, X., Yang, C., Long, B., Gai, Y., and Zhang, W.: The influences of ammonia on aerosol formation in the ozonolysis of styrene: Roles of Criegee intermediate reactions, R. Soc. Open Sci., 5, 172171, 10.1098/rsos.172171, 2018b.

Malecha, K. T., and Nizkorodov, S. A.: Photodegradation of secondary organic aerosol particles as a source of small, oxygenated volatile organic compounds, Environ Sci Technol, 50, 9990-9997, 10.1021/acs.est.6b02313, 2016.

Mandariya, A. K., Gupta, T., and Tripathi, S. N.: Effect of aqueous-phase processing on the formation and evolution of organic aerosol (OA) under different stages of fog life cycles, Atmos. Environ., 206, 60-71, 10.1016/j.atmosenv.2019.02.047, 2019.

Middlebrook, A. M., Bahreini, R., Jimenez, J. L., and Canagaratna, M. R.: Evaluation of composition-dependent collection efficiencies for the aerodyne aerosol mass spectrometer using field data, Aerosol Sci. Tech., 46, 258-271, 10.1080/02786826.2011.620041, 2012.

Moise, T., Flores, J. M., and Rudich, Y.: Optical properties of secondary organic aerosols and their changes by chemical processes, Chem. Rev., 115, 4400-4439, 10.1021/cr5005259, 2015.

Na, K., Song, C., Switzer, C., and Cocker, D. R.: Effect of ammonia on secondary organic aerosol formation from α-pinene ozonolysis in dry and humid conditions, Environ. Sci. Technol., 41, 6096-6102, 10.1021/es061956y, 2007.

Ng, N. L., Chhabra, P. S., Chan, A. W. H., Surratt, J. D., Kroll, J. H., Kwan, A. J., McCabe, D. C., Wennberg, P. O., Sorooshian, A., Murphy, S. M., Dalleska, N. F., Flagan, R. C., and Seinfeld, J. H.: Effect of NOx level on secondary organic aerosol (SOA) formation from the photooxidation of terpenes, Atmos. Chem. Phys., 7, 5159-5174, 10.5194/acp-7-5159-2007, 2007a.

Ng, N. L., Kroll, J. H., Chan, A. W. H., Chhabra, P. S., Flagan, R. C., and Seinfeld, J. H.: Secondary organic aerosol formation from m-xylene, toluene, and benzene, Atmos. Chem. Phys., 7, 3909-3922, 10.5194/acp-7-3909-2007, 2007b.

Ng, N. L., Canagaratna, M. R., Zhang, Q., Jimenez, J. L., Tian, J., Ulbrich, I. M., Kroll, J. H., Docherty, K. S., Chhabra, P. S., Bahreini, R., Murphy, S. M., Seinfeld, J. H., Hildebrandt, L., Donahue, N. M., DeCarlo, P. F., Lanz, V. A., Prévôt, A. S. H., Dinar, E., Rudich, Y., and Worsnop,

https://doi.org/10.5194/acp-2021-560
Preprint. Discussion started: 22 July 2021


Atmospheric Chemistry and Physics Discussions

688 D. R.: Organic aerosol components observed in Northern Hemispheric datasets from Aerosol
689 Mass Spectrometry, Atmos. Chem. Phys., 10, 4625-4641, 10.5194/acp-10-4625-2010, 2010.

690 Ng, N. L., Brown, S. S., Archibald, A. T., Atlas, E., Cohen, R. C., Crowley, J. N., Day, D. A.,
691 Donahue, N. M., Fry, J. L., Fuchs, H., Griffin, R. J., Guzman, M. I., Herrmann, H., Hodzic, A.,
692 Iinuma, Y., Jimenez, J. L., Kiendler-Scharr, A., Lee, B. H., Luecken, D. J., Mao, J., McLaren, R.,
693 Mutzel, A., Osthoff, H. D., Ouyang, B., Picquet-Varrault, B., Platt, U., Pye, H. O. T., Rudich, Y.,
694 Schwantes, R. H., Shiraiwa, M., Stutz, J., Thornton, J. A., Tilgner, A., Williams, B. J., and Zaveri,
695 R. A.: Nitrate radicals and biogenic volatile organic compounds: oxidation, mechanisms, and
696 organic aerosol, Atmos. Chem. Phys., 17, 2103-2162, 10.5194/acp-17-2103-2017, 2017.

697 Nguyen, T. B., Laskin, A., Laskin, J., and Nizkorodov, S. A.: Brown carbon formation from
698 ketoaldehydes of biogenic monoterpenest, Faraday Discuss., 165, 473-494, 10.1039/c3fd00036b,
699 2013.

700 NIST: NIST Chemistry WebBook Standard Reference Database 69,
701 https://doi.org/10.18434/T4D303, 2020.

702 Nozière, B., Dziedzic, P., and Cordova, A.: Products and kinetics of the liquid-phase reaction of
703 glyoxal catalyzed by ammonium ions (NH_4^+), J. Phys. Chem. A, 113, 231-237,
704 10.1021/jp8078293, 2009.

705 Ortiz-Montalvo, D. L., Hakkinen, S. A., Schwier, A. N., Lim, Y. B., McNeill, V. F., and Turpin, B.
706 J.: Ammonium addition (and aerosol pH) has a dramatic impact on the volatility and yield of
707 glyoxal secondary organic aerosol, Environ. Sci. Technol., 48, 255-262, 10.1021/es4035667,
708 2014.

709 Paciga, A. L., Riipinen, I., and Pandis, S. N.: Effect of ammonia on the volatility of organic diacids,
710 Environ. Sci. Technol., 48, 13769-13775, 10.1021/es5037805, 2014.

711 Peng, C., Yang, F., Tian, M., Shi, G., Li, L., Huang, R. J., Yao, X., Luo, B., Zhai, C., and Chen, Y.:
712 Brown carbon aerosol in two megacities in the Sichuan Basin of southwestern China: Light
713 absorption properties and implications, Sci. Total Environ., 719, 137483,
714 10.1016/j.scitotenv.2020.137483, 2020.

715 Qi, X., Zhu, S., Zhu, C., Hu, J., Lou, S., Xu, L., Dong, J., and Cheng, P.: Smog chamber study of
716 the effects of NOx and NH_3 on the formation of secondary organic aerosols and optical properties
717 from photo-oxidation of toluene, Sci. Total Environ., 727, 138632,
718 10.1016/j.scitotenv.2020.138632, 2020.

719 Sarrafzadeh, M., Wildt, J., Pullinen, I., Springer, M., Kleist, E., Tillmann, R., Schmitt, S. H., Wu,
720 C., Mentel, T. F., Zhao, D. F., Hastie, D. R., and Kiendler-Scharr, A.: Impact of NOx and OH on
721 secondary organic aerosol formation from β-pinene photooxidation, Atmos. Chem. Phys., 16,
722 11237-11248, 10.5194/acp-16-11237-2016, 2016.

723 Sun, Y. L., Zhang, Q., Schwab, J. J., Demerjian, K. L., Chen, W. N., Bae, M. S., Hung, H. M.,
724 Hogrefe, O., Frank, B., Rattigan, O. V., and Lin, Y. C.: Characterization of the sources and
725 processes of organic and inorganic aerosols in New York city with a high-resolution time-of-flight
726 aerosol mass apectrometer, Atmos. Chem. Phys., 11, 1581-1602, 10.5194/acp-11-1581-2011,

https://doi.org/10.5194/acp-2021-560
Preprint. Discussion started: 22 July 2021

2011.

Surratt, J. D., Murphy, S. M., Kroll, J. H., Ng, N. L., Hildebrandt, L., Sorooshian, A., Szmigielski, R., Vermeylen, R., Maenhaut, W., Claeys, M., Flagan, R. C., and Seinfeld, J. H.: Chemical composition of secondary organic aerosol formed from the photooxidation of isoprene, J. Phys. Chem. A, 110, 9665-9690, 10.1021/jp061734m, 2006.

Volkamer, R., Jimenez, J. L., San Martini, F., Dzepina, K., Zhang, Q., Salcedo, D., Molina, L. T., Worsnop, D. R., and Molina, M. J.: Secondary organic aerosol formation from anthropogenic air pollution: Rapid and higher than expected, Geophys. Res. Lett., 33, Artn L17811, 10.1029/2006gl026899, 2006.

Vu, T. V., Shi, Z., Cheng, J., Zhang, Q., He, K., Wang, S., and Harrison, R. M.: Assessing the impact of clean air action on air quality trends in Beijing using a machine learning technique, Atmos. Chem. Phys., 19, 11303-11314, 10.5194/acp-19-11303-2019, 2019.

Wang, R. Y., Ye, X. N., Liu, Y. X., Li, H. W., Yang, X., Chen, J. M., Gao, W., and Yin, Z.: Characteristics of atmospheric ammonia and its relationship with vehicle emissions in a megacity in China, Atmos. Environ., 182, 97-104, 10.1016/j.atmosenv.2018.03.047, 2018.

Wang, S. W., Zhang, Q., Martin, R. V., Philip, S., Liu, F., Li, M., Jiang, X. T., and He, K. B.: Satellite measurements oversee China's sulfur dioxide emission reductions from coal-fired power plants, Environ. Res. Lett., 10, 114015, 10.1088/1748-9326/10/11/114015, 2015.

Wang, X., Gao, S., Yang, X., Chen, H., Chen, J., Zhuang, G., Surratt, J. D., Chan, M. N., and Seinfeld, J. H.: Evidence for high molecular weight nitrogen-containing organic salts in urban aerosols, Environ. Sci. Technol., 44, 4441-4446, 10.1021/es1001117, 2010.

Wang, Y., Chen, Y., Wu, Z., Shang, D., Bian, Y., Du, Z., Schmitt, S. H., Su, R., Gkatzelis, G. I., Schlag, P., Hohaus, T., Voliotis, A., Lu, K., Zeng, L., Zhao, C., Alfarra, M. R., McFiggans, G., Wiedensohler, A., Kiendler-Scharr, A., Zhang, Y., and Hu, M.: Mutual promotion between aerosol particle liquid water and particulate nitrate enhancement leads to severe nitrate-dominated particulate matter pollution and low visibility, Atmos. Chem. Phys., 20, 2161-2175, 10.5194/acp-20-2161-2020, 2020.

Xia, Y., Zhao, Y., and Nielsen, C. P.: Benefits of China's efforts in gaseous pollutant control indicated by the bottom-up emissions and satellite observations 2000-2014, Atmos. Environ., 136, 43-53, 10.1016/j.atmosenv.2016.04.013, 2016.

Xie, M., Chen, X., Hays, M. D., Lewandowski, M., Offenberg, J., Kleindienst, T. E., and Holder, A. L.: Light absorption of secondary organic aerosol: composition and contribution of nitroaromatic compounds, Environ. Sci. Technol., 51, 11607-11616, 10.1021/acs.est.7b03263, 2017.

Xu, J., Huang, M. Q., Cai, S. Y., Liao, Y. M., Hu, C. J., Zhao, W. X., Gu, X. J., and Zhang, W. J.: Chemical composition and reaction mechanisms for aged p-xylene secondary organic aerosol in the presence of ammonia, J. Chin. Chem. Soc., 65, 578-590, 10.1002/jccs.201700249, 2018.

Xu, L., Kollman, M. S., Song, C., Shilling, J. E., and Ng, N. L.: Effects of NOx on the volatility of secondary organic aerosol from isoprene photooxidation, Environ. Sci. Technol., 48, 2253-2262, 10.1021/es404842g, 2014.

https://doi.org/10.5194/acp-2021-560
Preprint. Discussion started: 22 July 2021

Atmospheric Chemistry and Physics Discussions

766 Xu, L., Moller, K. H., Crounse, J. D., Kjaergaard, H. G., and Wennberg, P. O.: New insights into the
767 radical chemistry and product distribution in the OH-initiated oxidation of benzene, Environ. Sci.
768 Technol., 54, 13467-13477, 10.1021/acs.est.0c04780, 2020.

769 Yang, W. Y., Li, J., Wang, M., Sun, Y. L., and Wang, Z. F.: A case study of investigating secondary
770 organic aerosol formation pathways in Beijing using an observation-based SOA box model,
771 Aerosol Air Qual. Res., 18, 1606-1616, 10.4209/aaqr.2017.10.0415, 2018.

772 Yang, Y., Vance, M., Tou, F. Y., Tiwari, A., Liu, M., and Hochella, M. F.: Nanoparticles in road dust
773 from impervious urban surfaces: distribution, identification, and environmental implications,
774 Environ Sci-Nano, 3, 534-544, 10.1039/c6en00056h, 2016.

775 Yang, Z., Tsona, N. T., Li, J., Wang, S., Xu, L., You, B., and Du, L.: Effects of NOx and SO_2 on the
776 secondary organic aerosol formation from the photooxidation of 1,3,5-trimethylbenzene: A new
777 source of organosulfates, Environ. Pollut., 264, 114742, 10.1016/j.envpol.2020.114742, 2020.

778 Zhang, L., Wang, Y., Feng, C., Liang, S., Liu, Y., Du, H., and Jia, N.: Understanding the industrial
779 NOx and SO_2 pollutant emissions in China from sector linkage perspective, Sci. Total Environ.,
780 770, 145242, 10.1016/j.scitotenv.2021.145242, 2021.

781 Zhang, Q., Jimenez, J. L., Canagaratna, M. R., Ulbrich, I. M., Ng, N. L., Worsnop, D. R., and Sun,
782 Y.: Understanding atmospheric organic aerosols via factor analysis of aerosol mass spectrometry:
783 a review, Anal. Bioanal. Chem., 401, 3045-3067, 10.1007/s00216-011-5355-y, 2011.

784 Zhang, R., Wang, G., Guo, S., Zamora, M. L., Ying, Q., Lin, Y., Wang, W., Hu, M., and Wang, Y.:
785 Formation of urban fine particulate matter, Chem. Rev., 115, 3803-3855,
786 10.1021/acs.chemrev.5b00067, 2015.

787 Zhao, D. F., Schmitt, S. H., Wang, M. J., Acir, I. H., Tillmann, R., Tan, Z. F., Novelli, A., Fuchs, H.,
788 Pullinen, I., Wegener, R., Rohrer, F., Wildt, J., Kiendler-Scharr, A., Wahner, A., and Mentel, T. F.:
789 Effects of NOx and SO_2 on the secondary organic aerosol formation from photooxidation of α-
790 pinene and limonene, Atmos. Chem. Phys., 18, 1611-1628, 10.5194/acp-18-1611-2018, 2018.

791

792

https://doi.org/10.5194/acp-2021-560
Preprint. Discussion started: 22 July 2021

Atmospheric Chemistry and Physics Discussions

Tables

Table 1. Summary of experimental conditions in this study.

No.	Toluene (ppb)	H_2O_2 (ppm)	NH_3 (ppb)	NO_2 (ppb)	RH (%)	T (℃)	SOA mass conc. (μg m^{-3})
Exp.1	790	1.98	-	-	25±1	20±1	637±14.6
Exp.2	790	1.98	200	-	23±1	20±1	867±12.7
Exp.3	790	1.98	200	62	26±1	20±1	1020±10.6
Exp.4	790	1.98	-	63	25±1	20±1	452±18.9

Figures

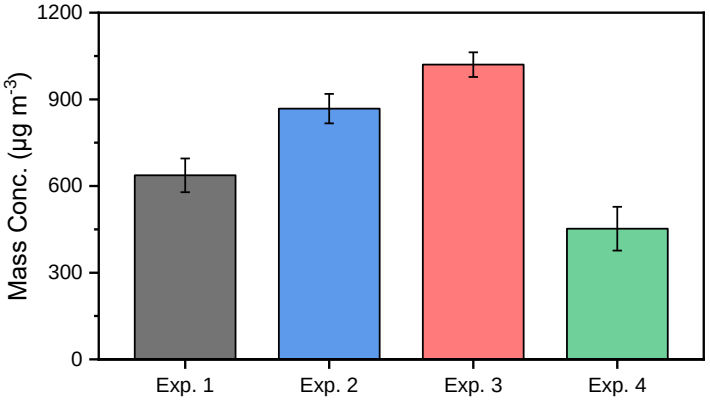

Fig. 1. Maximum mass concentration of toluene-derived SOA in different experiments. All the mass concentrations were wall-loss corrected.

https://doi.org/10.5194/acp-2021-560
Preprint. Discussion started: 22 July 2021

Atmospheric Chemistry and Physics Discussions

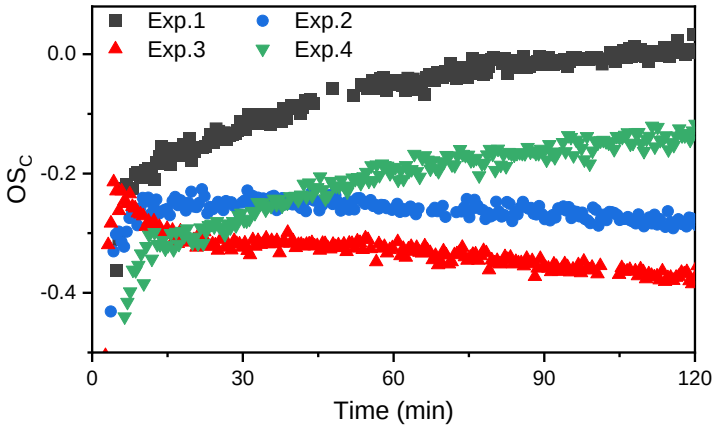

802

803 **Fig. 2.** The OS_C values for the toluene SOA formed under different NH_3/NOx conditions.

804

805

806

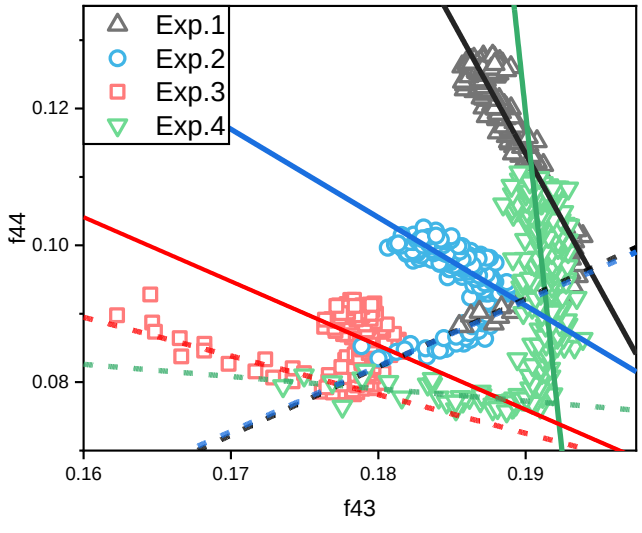

807

808 **Fig. 3.** The relationship between total organic signals at 43 m/z (f43) *vs.* 44 m/z (f44) from SOA
809 data during the photooxidation process. The f43 *vs.* f44 plots exhibited inflection points during the
810 photooxidation process. The dashed lines indicate the trends of f43 *vs.* f44 for the SOA formation
811 stage (before the inflection point) and the solid lines for the stable stage.

812

https://doi.org/10.5194/acp-2021-560
Preprint. Discussion started: 22 July 2021

Atmospheric Chemistry and Physics Discussions

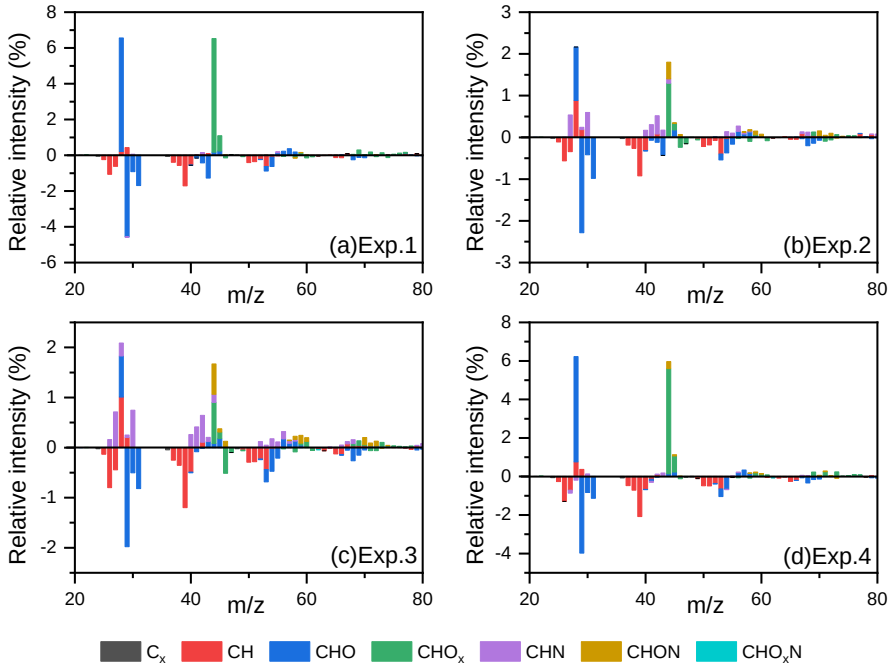

Fig. 4. The differential spectra of toluene SOA in the formation and stable stages. Data were taken and analyzed at a high resolution but were summarized to a unit mass resolution for display.

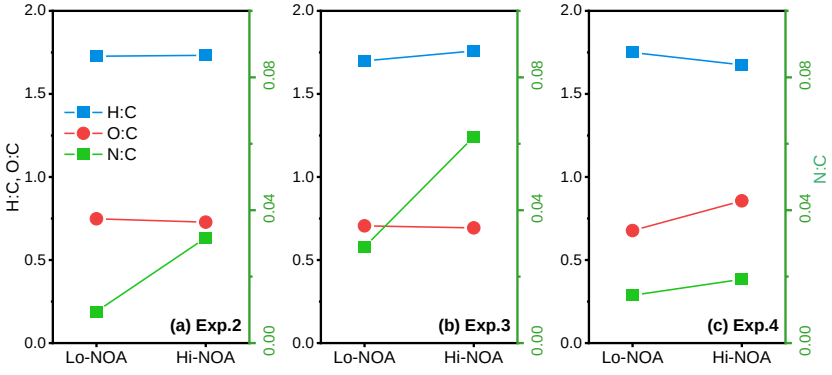

Fig. 5. The H/C, O/C, and N/C values of Hi-NOA and Lo-NOA for each experiment. (a) Exp. 2 with 200 ppb NH_3, (b) Exp. 3 with 200 ppb NH_3 and 62 ppb NO_2, and (c) Exp.4 with 63 ppb NO_2.

https://doi.org/10.5194/acp-2021-560
Preprint. Discussion started: 22 July 2021

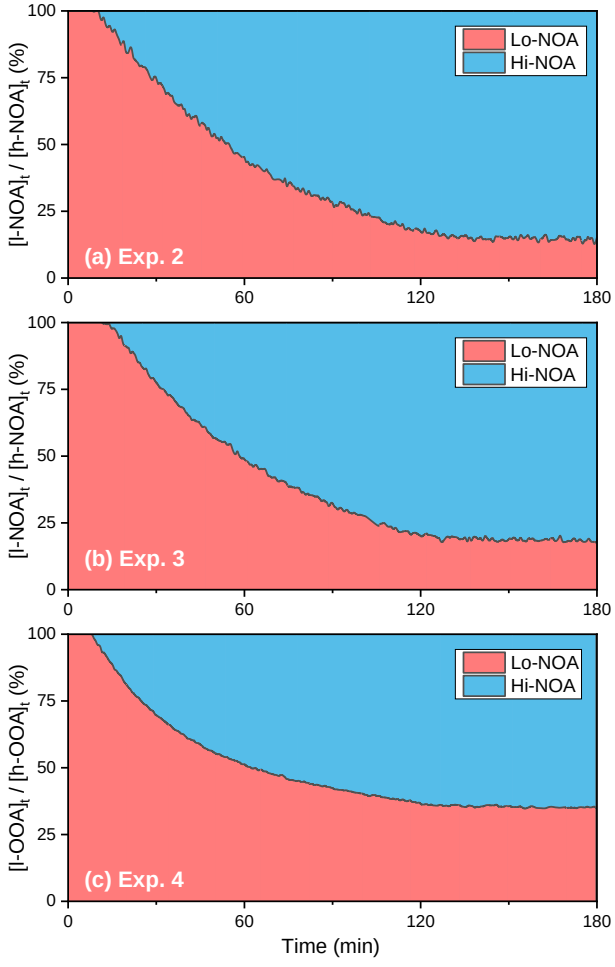

Fig. 6. The evolution of high-nitrogen OA (Hi-NOA) and low-nitrogen OA (Lo-NOA) during the photooxidation process under different NOx/NH_3 concentrations. Hi-NOA and Lo-NOA were not consistent among experiments. (a) Exp. 2 with 200 ppb NH_3, (b) Exp. 3 with 200 ppb NH_3 and 62 ppb NO_2, and (c) Exp. 4 with 63 ppb NO_2.

https://doi.org/10.5194/acp-2021-560
Preprint. Discussion started: 22 July 2021

Atmospheric Chemistry and Physics Discussions

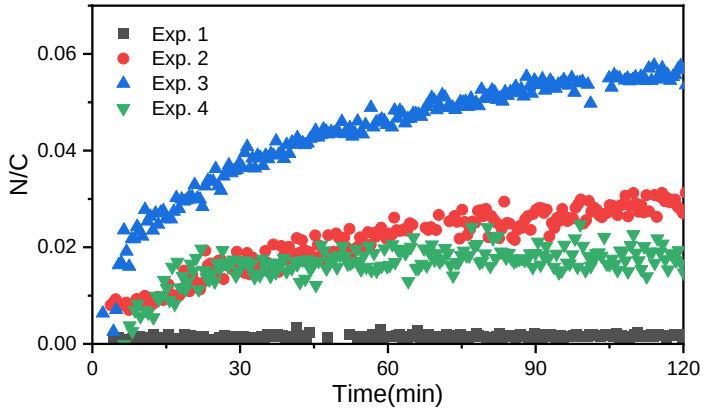

828

829 **Fig. 7.** The evolution of N/C in different experiments.

830

831

832

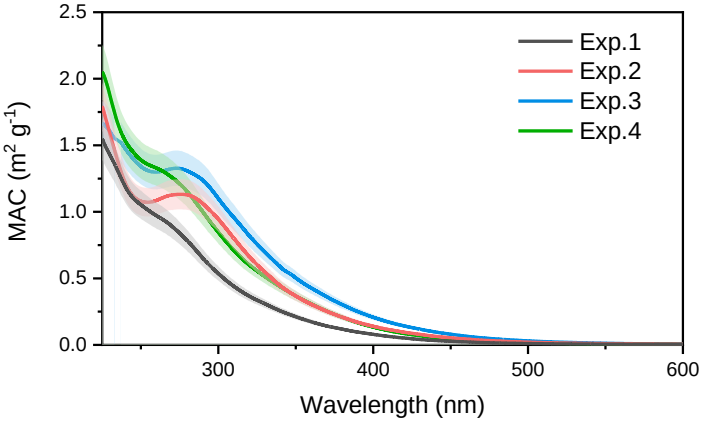

833

834 **Fig. 8.** The MAC over the range of 200–600 nm for the toluene SOA formed under different
835 experiment conditions.

836